

Synthesis and patterning of graphene: Strategies and prospects

Cite as: Appl. Phys. Rev. **6**, 021311 (2019); doi: [10.1063/1.5055624](https://doi.org/10.1063/1.5055624)

Submitted: 8 September 2018 · Accepted: 22 March 2019 ·

Published Online: 3 May 2019



View Online



Export Citation



CrossMark

Shobha Shukla,^{1,a)}  Seung-Yeon Kang,² and Sumit Saxena¹ 

AFFILIATIONS

¹Nanostructures Engineering and Modeling Laboratory, Department of Metallurgical Engineering and Materials Science, Indian Institute of Technology Bombay, Mumbai 400076, Maharashtra, India

²Department of Mechanical and Aerospace Engineering, Princeton University, Princeton, New Jersey 08544, USA

^{a)}Author to whom correspondence should be addressed: sshukla@iitb.ac.in

ABSTRACT

The extraordinary success of graphene in various applications has led to the quest to innovate techniques for production and patterning of nanomaterials. Numerous techniques such as vapor deposition, epitaxial growth, mechanical and chemical exfoliation have been explored to achieve this goal. These new methods have enabled the synthesis of a monolayer to a few layer graphene structures, in various forms such as films, nanoribbons, and 3D nanocomposites that are dispersed in solutions, suspended or deposited on substrates. However, several challenges still exist in processing graphene for futuristic device fabrication. Thus, there is a need to review the traditional processing and synthesis techniques developed for obtaining graphene. This review will provide a solid foundation on technology development for achieving economical and high throughput synthesis of high quality graphene for scalable applications. In this review, we provide a brief discussion on the theory of graphene, discuss synthesis techniques along with conventional and recent approaches to pattern graphene structures, and conclude with an emphasis on direct patterning methods. Discussions on the properties of graphene produced using different techniques and their emerging applications will assist in selecting an appropriate methodology for achieving desired properties in graphene. This is expected to be instrumental in the development of new strategies for fabrication of futuristic graphene-based devices.

Published under license by AIP Publishing. <https://doi.org/10.1063/1.5055624>

TABLE OF CONTENTS

I. INTRODUCTION	1
II. SYNTHESIS OF GRAPHENE.....	3
A. Cleavage/exfoliation of graphite to graphene	3
B. Chemical vapor deposition techniques for	
graphene synthesis	4
C. Epitaxial growth of graphene	4
D. Wet processes in synthesis of graphene	5
E. Photoexfoliation of graphene.....	5
F. Self-assembly of graphene	6
III. PATTERNING OF GRAPHENE.....	6
A. Inkjet printing.....	6
B. Standard photolithography	7
C. E-beam lithography/scanning probe microscopy/	
etching	9
D. Focused ion-beam (FIB) lithography.....	9
E. Self-assembly	10
F. Direct laser lithography	11
IV. CONCLUSION.....	12

V. OUTLOOK.....

I. INTRODUCTION

Discovery of graphene is considered as one of the major breakthroughs particularly in the area of materials science due to its unique properties. It is a two-dimensional sheet of carbon atoms in a honeycomb arrangement. The peculiar structure and presence of long-range order in such 2D materials have long been an area of active interest. This appeals for a brief discussion of travel in time on the exploration of 2D materials.

2D materials typically refer to monolayered crystalline materials with a long-range order. The plausibility of realization of such materials with a long range order was ruled out by Peierls¹ in the early 1990s based on qualitative arguments. Peierls' arguments were supported by Landau's general theory of second-order phase transitions.² Furthering these arguments, Mermin in 1968 showed that for a classical system containing N particles interacting via pair potentials of Lennard-Jones type, crystalline long-range order is not feasible.³ The findings of Mermin, however, were inconclusive for hard core

potentials. These theoretical predictions seemed in tune with the experimental observation of lowering in melting temperature with the sample thickness. The only hope to observe such a long-range 2D order was associated with hypothetical materials which could be described within the harmonic approximation. Several efforts were made to explore such layered materials.

The earliest accounts of realization of highly lamellar structures of thermally reduced graphite oxide can be accredited to Benjamin C. Brodie, as early as 1859. However, a major breakthrough in realization of 2D materials was provided by Geim and Novoselov in 2004, who successfully exfoliated monolayers of graphite by mechanical exfoliation using Scotch tape.⁴ One of the primary reasons for facilitation of this discovery was the subtle optical effects which graphene creates on top of a specific SiO₂ surface, making graphene optically “visible.” This discovery catalyzed the study and realization of novel 2D materials as these materials are predicted to demonstrate a plethora of new exotic properties. These members of 2D flatlands may be used as “Lego bricks” to design and fabricate quasi-2D hetero-structures to further tune their effective properties. 2D materials can be classified as elemental or compound based on their chemical compositions. Figure 1 shows a representative flatland of various 2D materials which have been investigated in the recent past.⁵

Of all the 2D materials explored, graphene is one of the most investigated materials to date. Structurally, graphene can be visualized as a monoatomic layer of sp² carbon atoms arranged on a honey comb lattice. This can also be described as two interpenetrating triangular sublattices. This sp² hybridization between one s and two p orbitals in the xy plane results in a planar geometry via formation of a σ bond. The σ bonds in graphene are robust and stronger as compared to the C-C bonds in diamond, thus forming one of the most stable materials known. The pure Pz orbital, normal to the graphene lattice binds covalently, forming π bonds which are half filled. These half-filled orbitals are known to show a strong tight binding character and have large Columbic energies, leading to strong collective effects in strongly correlated systems. The preliminary estimation of the electronic structure

of graphene using the tight binding approach was provided by Wallace in 1947,⁶ which was intended to understand the properties of bulk graphite. The band structure studies suggested that graphene is a semimetal with a linear band dispersion forming Dirac cones at the zone boundary.⁷ The Dirac fermions move with Fermi velocity ~300 times slower as compared to the speed of light in graphene. The availability of low energy linear dispersion in graphene resembles the physics of quantum electrodynamics (QED) for massless fermions, and hence, graphene offers a playground for QED effects at much lower speeds.^{8–10} Other interesting phenomena associated with the linear band dispersion are the Klein Paradox⁹ and the phenomenon of Zitterbewegung.¹¹ In addition to exhibiting exotic physical effects arising from its linear low energy dispersion, graphene also shows ballistic transport properties. The ballistic transport effect enables the electrons to propagate over long distances at times up to the order of micrometers without scattering. This makes graphene an excellent electrical and thermal conductor finding numerous applications in field effect devices,¹² spin injection devices,¹³ and others. Other potential applications of graphene include water quality sensing,¹⁴ water purification,^{15,16} field emission devices,¹⁷ and gas and biosensors.¹⁴ The adsorption/absorption of these molecules on the surface results in the change in the conductivity of graphene.¹⁸ The optical properties of graphene supported by ballistic transport make graphene a potential candidate for replacing transparent ITO/FTO coatings for making transparent contacts in photodevices and displays.^{19–21} A plethora of multidisciplinary applications along with exotic properties of graphene warrants a detailed discussion on its synthesis methodology.

Before proceeding to discuss various synthesis methodologies, it is important to note that graphene, in theory, is a planar one-atom thick layer. The literature suggests that the electronic structure of graphene changes rapidly with the number of layers and approaches the 3D limit of graphite at the thickness of ~10 graphene layers.^{22,23} Only graphene and a bilayer graphene can be considered as zero-gap semiconductors, and as for three or more layers, the spectra become increasingly complicated.^{4,22–24} In this paper, the term graphene will

Graphene family	Graphene	hBN ‘white graphene’		BCN	Fluorographene	Graphene oxide
2D chalcogenides	MoS ₂ , WS ₂ , MoSe ₂ , WSe ₂		Semiconducting dichalcogenides: MoTe ₂ , WTe ₂ , ZrS ₂ , ZrSe ₂ and so on		Metallic dichalcogenides: NbSe ₂ , NbS ₂ , TaS ₂ , TiS ₂ , NiSe ₂ and so on	
					Layered semiconductors: GaSe, GaTe, InSe, Bi ₂ Se ₃ and so on	
2D oxides	Micas, BSCCO	MoO ₃ , WO ₃		Perovskite-type: LaNb ₂ O ₇ , (Ca,Sr) ₂ Nb ₃ O ₁₀ , Bi ₄ Ti ₃ O ₁₂ , Ca ₂ Ta ₂ TiO ₁₀ and so on		Hydroxides: Ni(OH) ₂ , Eu(OH) ₂ and so on
	Layered Cu oxides	TiO ₂ , MnO ₂ , V ₂ O ₅ , TaO ₃ , RuO ₂ and so on				Others

FIG. 1. Schematic showing library of recently explored 2D materials. Reproduced with permission from Geim and Grigorieva, Nature 499, 419 (2013). Copyright 2013 Springer Nature.

TABLE I. Summary of various techniques highlighting their advantages and limitations used for synthesizing graphene.

Technology	Advantages	Limitations
Mechanical cleavage/exfoliation “Scotch tape method”	Simple Pristine single layer to few layer graphene	Lab-scale production Additional transferring step to a substrate
Liquid phase cleavage/exfoliation	Cost-effective	Careful selection and handling of chemicals
Chemical vapor deposition (CVD)	Pristine single layer to few layer graphene possible Can provide patterned growth of graphene	Slow process Restricted choice in substrates
Epitaxial growth	Large area growth Pristine single layer to few layer graphene Can provide patterned growth of graphene	Expensive Slow process Restricted choice in substrates
Wet process growth	Cost-effective Suitable for mass production	Expensive Difficult graphene quality control Careful selection and handling of chemicals
Photoexfoliation	Pristine single layer to few layer graphene	Small scale
Self-assembly	Pristine single layer to few layer graphene	Involves multiple steps, such as polymerization, carbonization, and chemical removal, etc.

include mono- and few-layer graphene (FLG), and multilayer graphene structures that may be slightly thicker than FLGs.

II. SYNTHESIS OF GRAPHENE

One of the earliest attempts to synthesize graphene was made by Bang in 1975²⁵ by thermal decomposition of ethylene on heated platinum substrates. However, the inability to identify the potential of this wonder material did not generate sufficient scientific enthusiasm. Other scattered attempts to synthesize graphene were made subsequently by cracking ethylene on the TiC (111) surface²⁶ and exfoliation of graphite by intercalation.²⁷ In this pursuit, first repeatable synthesis of graphene has been credited to Novoselov *et al.*⁴

Currently, there are many approaches to synthesize graphene that ranges from reduction of graphene oxide to directly growing graphene. Various synthesis methods and their unique features are discussed in this section, and Table I lists the advantages and limitations arising from each of these techniques.

A. Cleavage/exfoliation of graphite to graphene

Graphite can be considered as stacked sheets of graphene interacting via weak van der Waals forces. The layered structure with interlayer separation of $\sim 3.3 \text{ \AA}$ allows graphite to be intercalated by diffusion of intercalant particles between the layers as shown in the schematic in Fig. 2. The intercalation results in expansion of the graphite lattice along the “c” axis resulting in further weakening of the graphene interlayer interactions.^{27,28} This results in exfoliation of

graphene sheets. These sheets however roll to form nanoscrolls when sonicated. The microscopic analysis of the results showed formation of ~ 40 layers which are slightly thicker than a few-layer-graphene (FLG). This method however suggested the feasibility and provided hope for synthesis of FLG or even graphene by simple exfoliation of graphite.

Soon after the synthesis of carbon nanoscrolls, Novoselov *et al.*⁴ in 2004 demonstrated a novel approach to synthesize few- and monolayer graphene by mechanical exfoliation instead of chemical exfoliation. In general, graphene can be exfoliated from graphite by applying normal or lateral forces.²⁹ This technique is classified as mechanical exfoliation of graphene. Figure 3 shows a step-by-step procedure for mechanically exfoliating graphite to obtain graphene sheets. In their study, Novoselov and co-workers took 1 mm thick sheet of highly oriented pyrolytic graphite (HOPG), dry etched it in oxygen plasma, placed it on a photoresist, and baked the samples. Graphene sheets were then exfoliated mechanically by using a Scotch-tape method. In this method, a Scotch tape is stuck to the surface of HOPG and is then peeled off. This results in adhesion of mono- and few layers of graphene sheets left on to the photoresist, which are then recovered using acetone. This micromechanical cleavage technique was scaled up in a lathe like experimental setup for synthesizing graphene flakes.³⁰

Liquid-phase exfoliation that uses hydrodynamic shear forces on graphitic substrates have also been used successfully to exfoliate graphene by dispersing them in solvents.³¹ In this technique, a careful choice of solvent is made so that the interfacial surface tension

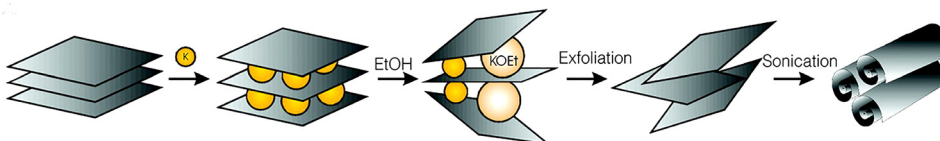


FIG. 2. Schematic of the intercalation/exfoliation process. Graphite is intercalated with potassium ions and then exfoliated using ethanol (EthOH) to form a dispersion of carbon sheets. In this process, sonication as a last step produces carbon nano-scrolls. Reproduced with permission from Vinculis *et al.*, Science **299**, 1361 (2003). Copyright 2003 The American Association for the Advancement of Science.

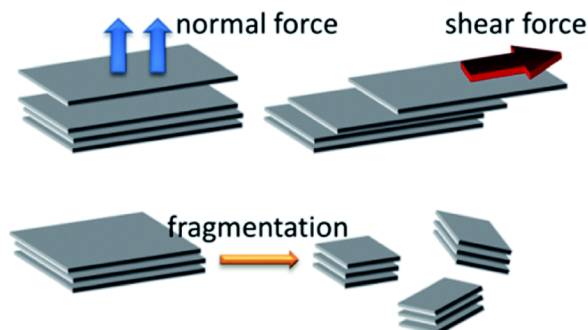


FIG. 3. Schematic showing micromechanical exfoliation of graphite using normal and shear forces to obtain graphene flakes. Reproduced with permission from Yi and Shen, *J. Mater. Chem. A* **3**, 11700 (2015). Copyright 2015 Royal Society of Chemistry.

between the graphene flakes and liquid is minimized to assist the dispersion of graphene flakes into the solvents and to ensure no chemical reaction is involved to prevent flakes turning into graphene oxide.^{32,33} The hydrodynamic forces produced in this technique are associated with the cavitation process. These forces are generated by formation, growth, and collapse of bubbles or voids during the ultrasonication process. The sample may further be cleaned to obtain FLG by ultracentrifuging the samples and surfactants or dispersing agents may be added to inhibit coagulation or sheet restacking due to van der Waals forces.^{31,32}

B. Chemical vapor deposition techniques for graphene synthesis

The chemical vapor deposition (CVD) technique involves a family of processes for growing materials on a solid surface. It involves flowing of gaseous precursor on a substrate in a chamber as shown in Fig. 4, resulting in a chemical reaction under appropriate environments. Different variations of CVD techniques include thermal chemical vapor deposition (thermal-CVD), plasma enhanced chemical vapor deposition (PECVD), cold wall and hot wall CVD, to name a few.

CVD has been used to synthesize a wide variety of materials, and graphene is no exception.³⁴ Copper (Cu) and Nickel (Ni) are known to catalyze chemical reactions in synthesis of carbon nanomaterials,

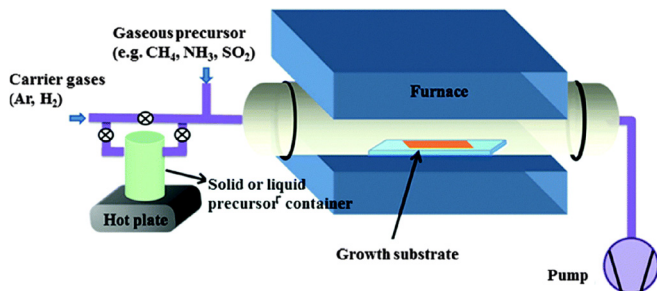


FIG. 4. A representative schematic of the basic setup for synthesis of graphene using the chemical vapor deposition technique. Reproduced with permission from Wang *et al.*, *Chem. Soc. Rev.* **43**, 7067 (2014). Copyright 2014 Royal Society of Chemistry.

thus forming a natural choice for substrates to be used in synthesis of graphene using the CVD technique. Reports on growth of single and multilayered graphene on Cu substrates at elevated temperatures can be traced back to 1991, while those on growth of graphitic materials on Ni substrates have been traced as early as 1966 when Karu and Beer reported synthesis of thin graphite by flowing Methane over Ni at 900 °C.³⁵ However, the grain size limitation on Ni is understood to be a bottleneck in synthesis of large area graphene. The modified CVD process on the Cu substrate by Li *et al.* resulted in successful growth of larger graphene sheets.³⁶

The CVD techniques incorporated with concentric tube (CT) reactors have led to the development of CTCVD techniques for roll to roll production of graphene films on copper foils. In this process, the substrate translates a helical path and is wrapped on a surface of quartz tube mounted concentrically within another quartz tube³⁷ as shown in Fig. 5. The reactor volume is determined by the annular gap between the coaxial tubes and the length over which the system is heated. This modified CVD technique has enabled in depositing very large graphene sheets on copper foils up to ~4 m length. The striations and defects in form of pits and surface roughness produced during the deposition process form detrimental factors in uniform coverage of the graphene sheets.

C. Epitaxial growth of graphene

Epitaxial growth of graphene has been achieved by catalytic decomposition of hydrocarbons on metal surfaces. One of the earliest accounts of deposition of graphitic multilayers on the Ni (111) surface at low temperatures (<1065 K) was reported by Shelton *et al.* in 1974.³⁸ However, at higher temperatures (~1065 K–1180K), the monolayer of graphite oriented epitaxially to the Ni surface was believed to have formed. This could not be verified due to the lack of sophisticated imaging techniques. The growth of monolayer graphite sheets/graphene is understood to occur due to desorption of oxygen or hydrogen on heated substrates.

Graphene has also been reportedly synthesized by heating the silicon carbide substrate (SiC). Although the lattice constants of SiC (~3.073 Å) and graphene (~2.46 Å) vary significantly, heating results in desorption of silicon from top layers. The carbon remnant atoms in this process arrange themselves in a hexagonal lattice, resulting in the formation of few layer graphene sheets. This growth may be attributed to the anisotropic nature of chemical bonds. The quality of graphene sheets produced depends on the surface termination of SiC substrates.^{39,40} Graphene films grown using the Si-faced substrates show

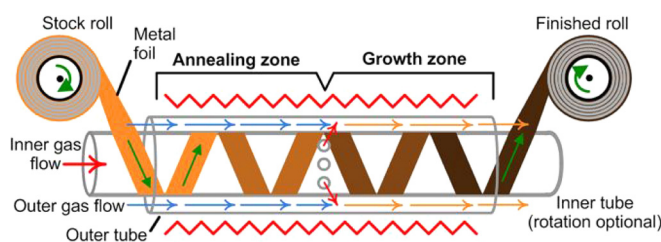


FIG. 5. Schematic showing roll to roll synthesis of graphene using the concentric tube chemical vapor deposition (CTCVD) technique on copper foil. Reproduced from Polsen *et al.*, *Sci. Rep.* **5**, 10257 (2015) Copyright 2015 Author(s), licensed under the Creative Commons Attribution 4.0 International License.

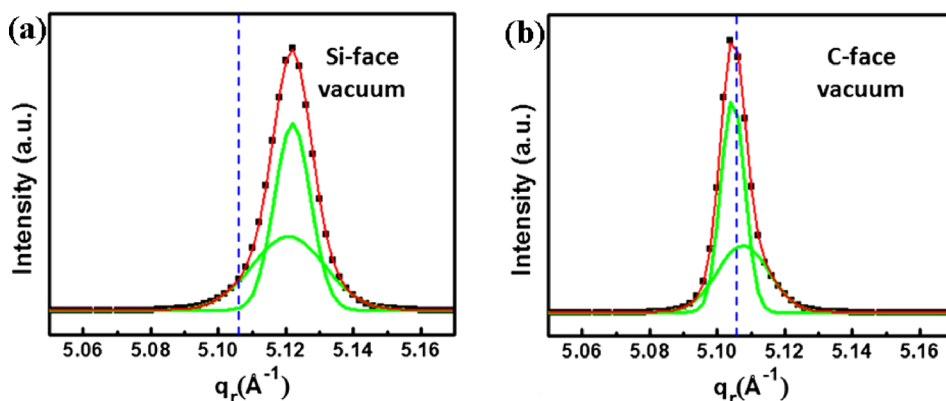


FIG. 6. Radial X-ray scan of the graphene samples produced from (a) Si terminated and (b) C terminated SiC substrates under vacuum. The blue dashed lines correspond to one half of the lattice constant of the unit cell in unstrained graphene. Reproduced with permission from Capano et al., *J. Mater. Res.* **29**, 439 (2014). Copyright 2014 Cambridge University Press.

larger long-range vertical order. The radial X-ray profiles shown in Fig. 6 suggest that larger grain sizes (an order of magnitude larger) of graphene sheets are produced when C-terminated SiC substrates are used.

D. Wet processes in synthesis of graphene

Wet chemical routes have also been explored to synthesize graphene. Some of the techniques used in these processes include chemical exfoliation by oxidation followed by reduction, unzipping of carbon nanotubes, and others. Of these, synthesis of graphene by chemical exfoliation followed by subsequent reduction is one of the most popular techniques. In this method, graphene oxide (GO)^{7,20} is produced by oxidation of graphite flakes.^{41,42} The oxidation of graphite flakes helps in exfoliation. Once exfoliated, these GO sheets can be dispersed in an aqueous medium. Another method to produce GO sheets is through the well-known Hummer's method which uses graphite flakes, sulphuric acid (H_2SO_4), sodium nitrate (NaNO_3), and potassium permanganate (KMnO_4).⁴¹ Subsequent reduction to graphene is achieved chemically through the use of strong reducing agents such as hydrazine or sodium borohydride and can also be achieved using thermal and electrochemical processes.⁴³ The schematic representation of this synthesis technique is shown in Fig. 7.⁴⁴ The graphene sheets so produced are not pristine and are defective. Hence, they are often called reduced graphene oxide (rGO) structures. Graphene plates obtained from exfoliation of graphite by means of an electrochemical process in inorganic salt-based electrolytes have also been reported to demonstrate properties similar to that of rGO structures.⁴⁵

Graphene is understood to be a precursor to most carbon nanostructures such as carbon nanotubes, nanoribbons, and nanocones. Another innovative technique demonstrated recently in pursuit to approach this problem is based on "unzipping" of carbon nanotubes

to form graphene nanoribbons. Three different methods that have been reportedly used to achieve this are based on intercalation followed by abrupt heating,⁴⁶ plasma etching,⁴⁷ and using multistep chemical treatment.⁴⁸

E. Photoexfoliation of graphene

Laser assisted photoprocesses have been explored to exfoliate graphene sheets from the graphite substrate. Irradiation of the laser with the target results in the detachment of an entire or a partial layer of the material, resulting in exfoliation/synthesis of small portions of two dimensional sheets or quantum dots.¹⁹ The physical process involved during the irradiation of the material by high energy laser pulses depends predominantly on the time duration of the interaction. The laser-material interactions in ultrashort durations (\sim femto-seconds) are different from those at longer timescales and are summarized in Fig. 8.⁴⁹

Pulsed lasers ranging from nanoseconds to femto-seconds have been used to ablate/exfoliate graphene sheets from the graphite target or other carbon precursors, using different wavelengths, repetition rates, and different operating environments. Most commonly used wavelengths for these processes are 1064 nm, 800 nm, and 532 nm.^{50,51} Figure 9 shows a TEM micrograph of one such 10 layered graphene sheet produced using laser exfoliation. The exact mechanism of the formation of graphene sheets and graphene quantum dots is not clearly understood. There have been several attempts to decouple thermal and nonthermal phenomena by changing ablation conditions, environments, and targets, but consensus could not be made for the best suitable condition for graphene synthesis using laser ablation processes.^{19,52} Some details involving the laser-graphene interaction from the patterning perspective will also be discussed in Sec. III F.

First principles calculations have shown that as the laser beam impinges the target, the topmost layer detaches. The propagation of

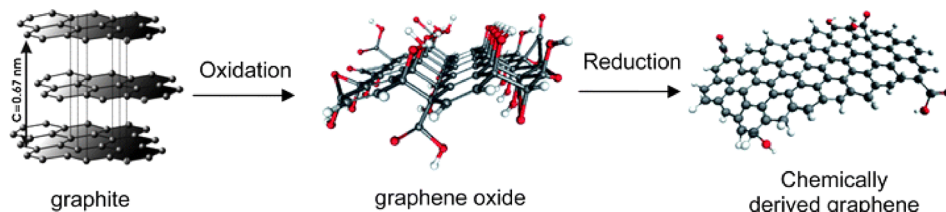


FIG. 7. Schematic representation of synthesis of graphene sheets by oxidation of graphite flakes followed by reduction of the graphene oxide sheets. Reproduced with permission from Zhang et al., *J. Mater. Chem.* **20**, 5983 (2010). Copyright 2010 Royal Society of Chemistry.

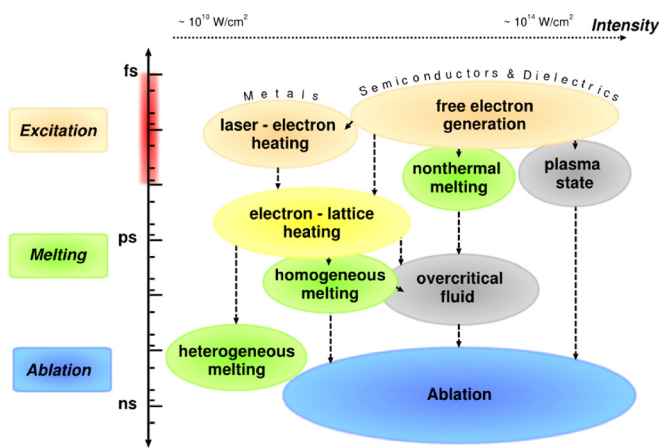


FIG. 8. Schematic showing the timescale dependence on various phenomena and processes in the laser-matter interaction. Reproduced from Rethfeld *et al.*, *J. Phys. D: Appl. Phys.* **50**, 193001 (2017). Copyright 2017 Author(s), licensed under the Creative Commons Attribution 3.0 License.

this effect is found to be slow, and much smaller structural changes are observed in subsurface layers.⁵³ Exfoliation of graphene using laser beams can be achieved at lower thresholds also if the van der Waals interaction can be reduced between the graphene layers.

F. Self-assembly of graphene

An inexpensive, self-assembly approach can be used to fabricate a single layer graphene sheet. In an experiment performed by Zhang *et al.*, Polypyrrole is used for self-assembling graphene layers. Polypyrrole serves as both a carbon precursor source and a surfactant for obtaining pure single-layer graphene sheets as shown in Fig. 10. A

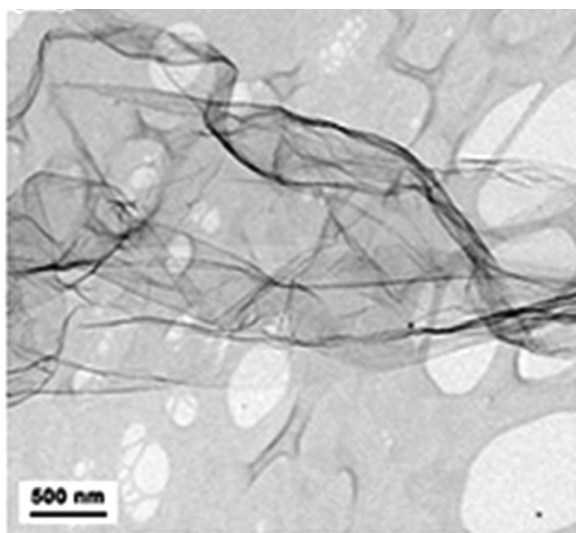


FIG. 9. TEM micrograph of exfoliated graphene sheets obtained using the pulsed Nd:YAG laser (Laser parameters used: 532 nm wavelength, 7 ns pulsewidth, and 1 Hz repetition rate). Reproduced with permission from Shukla and Saxena, *Appl. Phys. Lett.* **98**, 173108 (2011), Copyright 2011 AIP Publishing LLC.

structure-directing surfactant containing a Pyrrole moiety is used to construct lamellar meso-structured silica. During the formation of the lamellar silica framework, the Pyrrole moieties are densely packed in a controlled fashion within confined 2D spaces between silica layers. After a series of polymerization, carbonization, and silica shell removal processes, single-layer graphene sheets are obtained.⁵⁴ Graphene-composite foam has also been made by the incorporation of hydroxyapatite,⁵⁵ polystyrene,⁵⁶ and MoS₂⁵⁷ using self-assembly. Most of the self-assembly protocols use gelation for forming graphene 3D structures. All these self-assembly processes typically involve temperature dependent stacking.

III. PATTERNING OF GRAPHENE

Since the inception of graphene, many attempts have been made to pattern graphene for a wide variety of applications from graphene photonics, plasmonics, and broadband optoelectronic devices to supercapacitors.^{58,59} Graphene tends to change its properties with addition of every single layer of graphene. Applications of graphene vary depending on the layer thickness, quality of layers, quality of sp² structures, and the choice of substrate materials, which are all affected by the patterning technique used. Thus, patterning has been attempted for monolayers as well as multilayers and on suspended and nonsuspended substrates.

In this section, some of the standard and more recent techniques will be discussed starting with inkjet printing, standard photolithography, e-beam lithography, focused ion beam lithography, self-assembly, and direct laser lithography. Table II lists the advantages and limitations arising from each graphene patterning technique discussed in this section.

A. Inkjet printing

Inkjet printing, also referred to as nozzle printing, of graphene begins from the formulation of graphene ink via dispersing exfoliated graphene flakes or graphene oxide flakes in various solvents with additional chemicals such as surfactants, dispersants, various polymers, and conducting materials to help achieve the right viscosity, stability, and conductivity of the ink.^{60–64} Ink can be made with different graphene concentrations, which is then deposited through inkjet printing over a predefined area. Patterning is often followed by a high temperature annealing process if the pattern is printed with a graphene oxide ink.^{61,63,66} Although polymer stabilizer and surfactants enhance ink stability and printing performance, a postannealing step is required to remove the remaining polymer and to achieve optimal electrical properties of the printed patterns. Polymer decomposition using light annealing has also been reported in addition to the traditional thermal annealing.⁶⁴ Careful choice in solvent should be made to meet the required rheological parameters such as density, surface tension, and viscosity for an optimal ink-jet printing process.⁶⁵ The Inkjet printing technique is also widely investigated for 3D printing, and 3D-printed graphene aerogel structures and scaffolds have been successfully reported.^{66,67} Other available ink-based printing methods such as screen printing and spray printing have also been used to print graphene features.^{68,69} Santra *et al.* have developed a technique to fabricate humidity sensors by integrating the CMOS MEMS microhot plate with ink jet printed graphene as shown in Fig. 11. The graphene nanoplatelets appear as bright spots in Fig. 11(b) which allow the sensing by providing conducting paths. The conducting nature of graphene

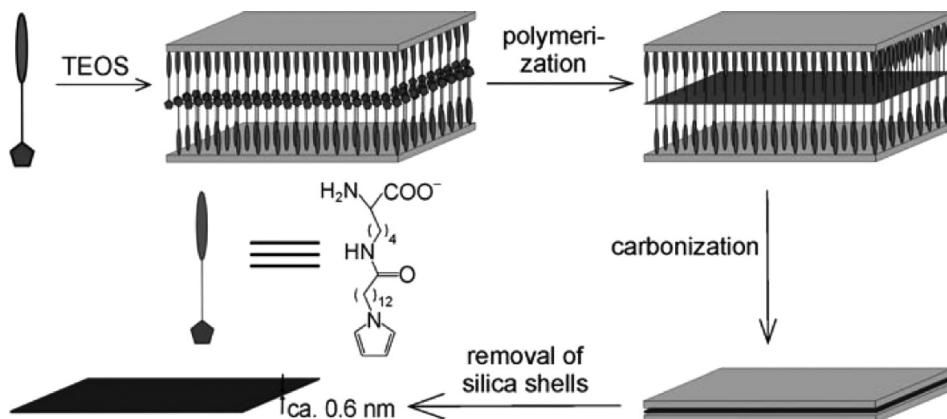


FIG. 10. Schematic representation of the fabrication of pure single-layer graphene with a thickness of about 0.6 nm. TEOS tetraethoxysilane. Reproduced with permission from Zhang *et al.*, Angew. Chem., Int. Ed. **48**, 5864 (2009). Copyright 2010 John Wiley and Sons.

platelets allows conduction of current electron hopping through the nonconducting polymer matrix. This electron hopping may arise from single or multistep hopping depending on interplatelet separation which in turn depends on the volume fraction of the graphene platelets in the ink.

The integrated CMOS MEMS microhot plate enables in controlling the temperature of the sensors and facilitating in temperature-

TABLE II. Summary of the advantages and limitations of graphene patterning techniques.

Technology	Advantages	Limitations
Ink-jet printing ^{60–69}	3D structures possible Direct patterning technique	Limited resolution
Photolithography ^{70–77}	Large areas High resolution Direct patterning technique	Multiple steps required Inherent 2D technique
Electron-beam, scanning probe lithography ^{74,78–80}	Very high resolution Direct patterning technique	Multiple steps required Inherent 2D technique Limited to small areas Expensive
FIB lithography ^{81–86}	Very high resolution Direct patterning technique	Slow in speed Inherent 2D technique Limited to small areas Expensive
Self-assembly ^{87–90}	Low in cost High quality 3D structures	Lacks patternability Difficult quality control
Direct laser lithography ^{51,52,91–101}	Direct patterning technique	Difficult quality control

dependent investigations of the humidity sensor. It is however observed that the increase in temperature of the sensor results in loss in sensitivity of the response of the sensor.

As another example, Zhu *et al.* fabricated periodic graphene aerogel microlattices using the direct ink writing technique. The GO inks used in this technique were prepared by mixing GO suspensions in the silica filler. The 3D objects were printed by extruding the GO ink from a micronozzle attached to the syringe barrel filled with ink. The entire process of 3D printing was performed in the bath of isooctane to avoid clogging of the micronozzle. Several structures including simple woodpile to complicated honeycomb structures were successfully fabricated as shown in Figs. 12(a)–12(f).

The properties of these 3D printed microlattices were found to enhance as compared to those of bulk aerogel materials. The fabricated 3D graphene microlattices demonstrated good electrical conductivity, low relative density, large surface area, and supercompressibility. Further, one could tune these properties by altering the GO ink formulation.

Incorporation of graphene flakes with biocompatible, biodegradable, and hyperelastic polymers to form graphene inks has led to exploration of this 3D printing technique for fabricating scaffolds. In a recent study, Jakus *et al.* have reported 3D printing of graphene scaffolds for biomedical applications. In addition to being biocompatible, these scaffolds are electrically conductive and mechanically resilient. Figure 13 shows different types of scaffolds fabricated using the direct ink writing technique.

Scaffolds fabricated using polymer based graphene inks have been used in *in-vitro* as well as *in-vivo* studies. These studies suggest that these 3D graphene are capable of supporting a variety of distinct cell types including the adult mesenchymal stem cells.

B. Standard photolithography

Standard photo-lithography techniques can be used to pattern graphene films.^{70–74} One such schematic is shown in Fig. 14. In general, a large area monolayer of graphene is prepared using CVD technique on metals, such as Cu and Pt. The most complex component in patterning of graphene structures through photo-lithography lies in the next transferring step. Various transfer technologies have been developed to transfer CVD grown graphene from metal growth substrates to device-compatible substrates to achieve a clean and crack-

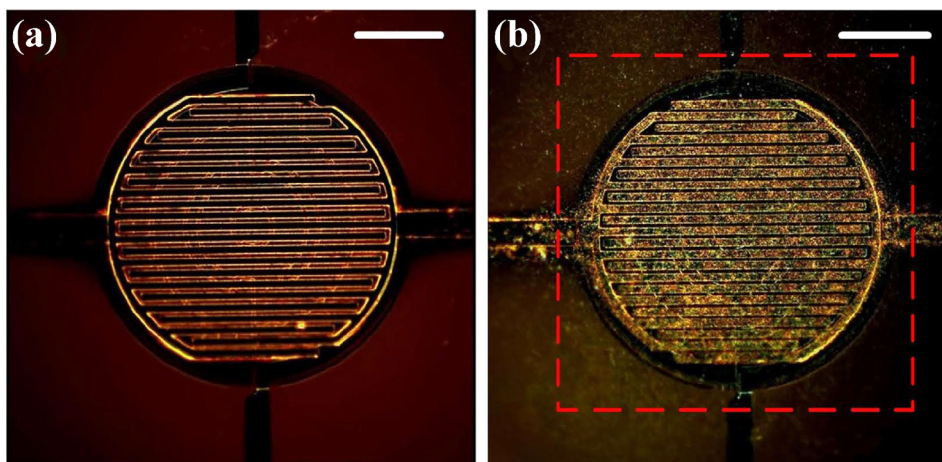


FIG. 11. Fabrication of interdigitated sensing electrodes (IDEs) through an ink-jet printing method. (a) Dark field optical microscopy image of the IDEs on the CMOS microhot plate without graphene and (b) with graphene-PVP deposited on to IDEs, with the targeted printing area marked by dashed lines. The scale bar is $100 \mu\text{m}$. Reproduced from Santra et al., Sci. Rep. 5, 17374 (2015) with Copyright 2015 Author(s), under the Creative Commons Attribution 4.0 International License.

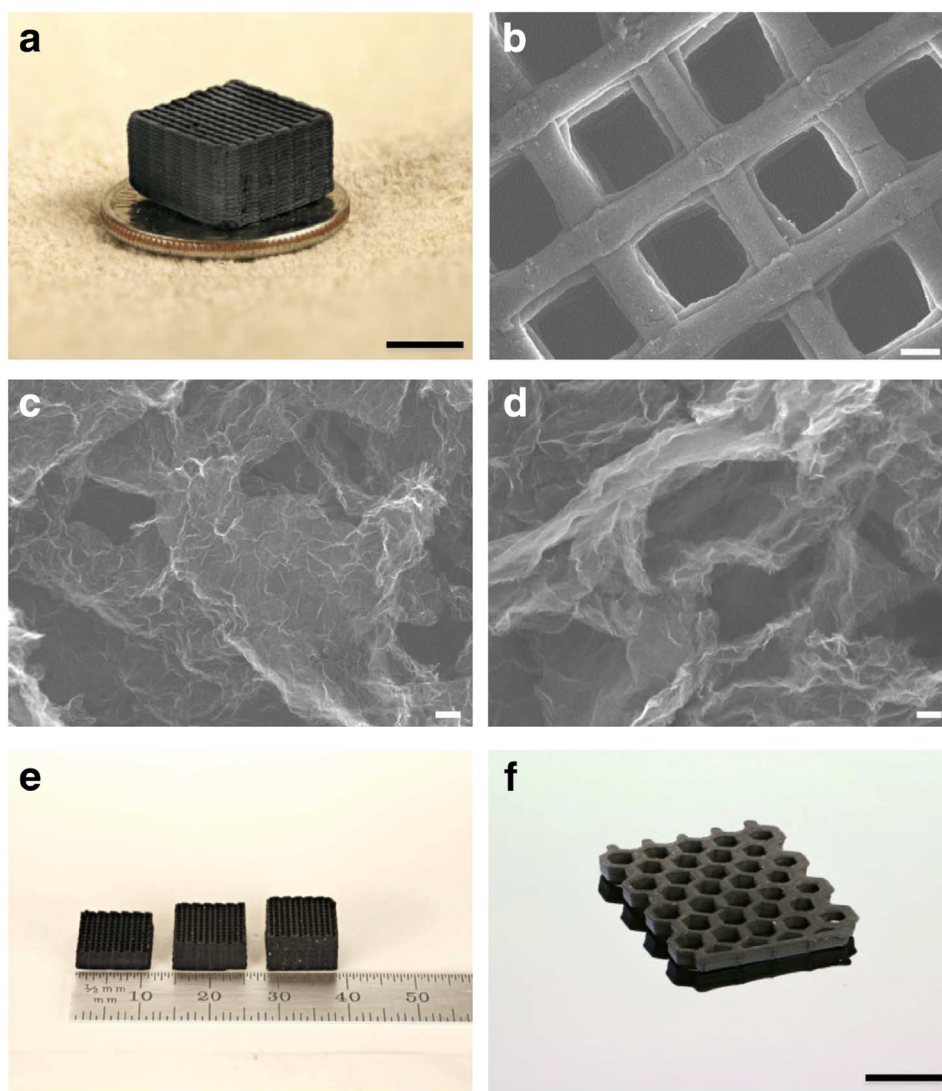


FIG. 12. 3D ink-jet printed graphene aerogels. (a) Optical image of a 3D printed graphene aerogel microlattice. SEM images of (b) 3D printed graphene aerogel microlattice, (c) graphene aerogel without resorcinol-formaldehyde solution (R-F) after etching and (d) graphene aerogel with 4 wt % R-F after etching. The R-F solution was used to build a more open, less crosslinked network structure which leads to changes such as density and conductivity. Optical image of (e) 3D printed graphene aerogel microlattices with varying thicknesses and (f) a 3D printed graphene aerogel honeycomb. Scale bars used in different figures are 5 mm (a), $200 \mu\text{m}$ (b), 100 nm (c) and (d), 1 cm (f). Reproduced from Zhu et al., Nat. Commun. 6, 6962 (2015) with Copyright 2015 Author(s), licensed under the Creative Commons Attribution 4.0 International License.

less transfer of the graphene layers.^{75–77} The following steps are straight forward and identical as in conventional photolithography where a standard photoresist is spin-coated on the surface, followed by a baking step then a UV patterning process with a patterned mask. After the developing step, a thin metallic layer is evaporated on to the pattern to function as an additional hard protection mask.⁷⁰ The film so formed comprises only organic compounds, and hence, a simple oxygen plasma etching step is required. The photolithography technique has a long history of development and is well established for commercial use. Therefore, it is often a preferred patterning method for larger patterns with features larger than tens of nanometers and is considered more easily applicable for a scale-up process.^{72,73}

C. E-beam lithography/scanning probe microscopy/etching

Electron-beam lithography scans a focused beam of electrons to pattern a desired geometry on a surface covered with an electron-sensitive film (i.e., e-beam resist). Several groups have reported graphene patterning through e-beam lithography.^{78,79} The primary advantage when compared with photolithography is that it allows patterning of sub-20 nm resolution features. The procedure is analogous to standard photolithography where an e-beam changes the solubility of the resist. This enables selective removal of either the exposed or nonexposed regions of the resist by immersing it in a developing solvent, followed by an oxygen plasma etching step. Compared to photolithography, the main difference lies in the use of a special e-beam resist. Figure 15 shows the SEM micrograph from one such report on e-beam defined graphene nanoribbons with palladium as electrodes. For graphene-based field-effect transistors (GFETs), scanning tunneling microscopy (STM) or other etching techniques have also been

explored to achieve even higher-resolution graphene nanoribbon structures.^{74,80} Graphene nanoribbons offer an adequate bandgap which makes them attractive for room temperature operation of such transistors. The energy bandgap induced from the confinement of graphene ribbon structures scales inversely with the ribbon width, and therefore, an atomic level precision is required.^{74,80} Tapasztó *et al.* have shown cutting of a single graphene layer by simultaneously applying a constant bias potential and moving the STM tip with constant velocity to etch a desired geometry down to 2.5 nm,⁸⁰ and Wang and Dai used additional gas phase etching chemistry to narrow the graphene ribbons down to less than 10 nm.⁷⁴

D. Focused ion-beam (FIB) lithography

FIB is widely used for site-specific removal and deposition of the material. Milling or sputtering is achieved through collisions of energetic Ga⁺ ions with the target atoms and/or a gas injection system that is incorporated to deliver gaseous precursors of metals and insulators close to the sample.⁸¹ Ga⁺ FIB techniques have been used to pattern multilayer and suspended graphene structures.^{82,83} More recently, there have been reports on patterning single or few-layer graphene structures on nonsuspended graphene substrates through the use of a helium-ion beam.^{81,84–86} While the use of Ga⁺ ions has been more conventional to fabricate smaller and thinner devices, the use of He ion FIB has become more prevalent now. The large mass of the Ga⁺ ions allows a high sputtering rate, which is beneficial for a large device fabrication, but this may be problematic for a more precise nanodevice fabrication and cause unnecessary damage in the underlying substrate or device.⁸¹ The He-ion beam can produce a subnanometer probe size on the sample and produce far fewer collision cascades, which result in a smaller interaction volume near the surface that allows patterning

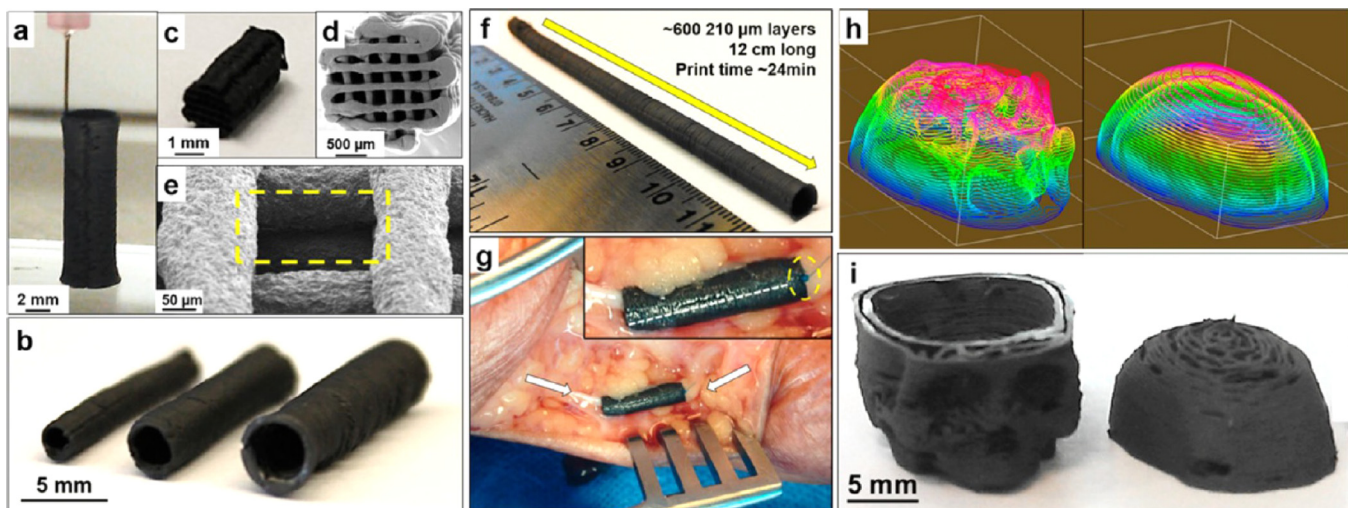


FIG. 13. 3D printed high-content graphene scaffolds for biomedical applications. (a) 3D-printed self-supporting tubular structures of (b) various sizes that could serve as custom-sized nerve graft conduits. (c) and (d) Uniaxial, multichannel nerve guides. (e) SEM micrograph of multichannel nerve conduit with every other layer close to contact (yellow box). (f) 3D-printed 5 mm diameter hollow tube structure composed of many hundreds of layers with a high aspect ratio 24:1, which can be cut to size as needed. (g) Photograph of tubular nerve conduit cut from (f) that was implanted into a human cadaver via longitudinal transection and wrapping around the ulnar nerve (white arrows). The nerve conduit was then sutured closed along the previously described longitudinal transection (white dotted line) as well as to the surrounding epineurium and nerve tissue (inset, yellow circle). (h) Digitally sliced STL file of the skull and skull cap and (i) photograph of the resulting 3D-printed skull and skull cap. Reproduced with permission from Jakus *et al.*, ACS Nano 9, 4636 (2015). Copyright 2015 American Chemistry Society.

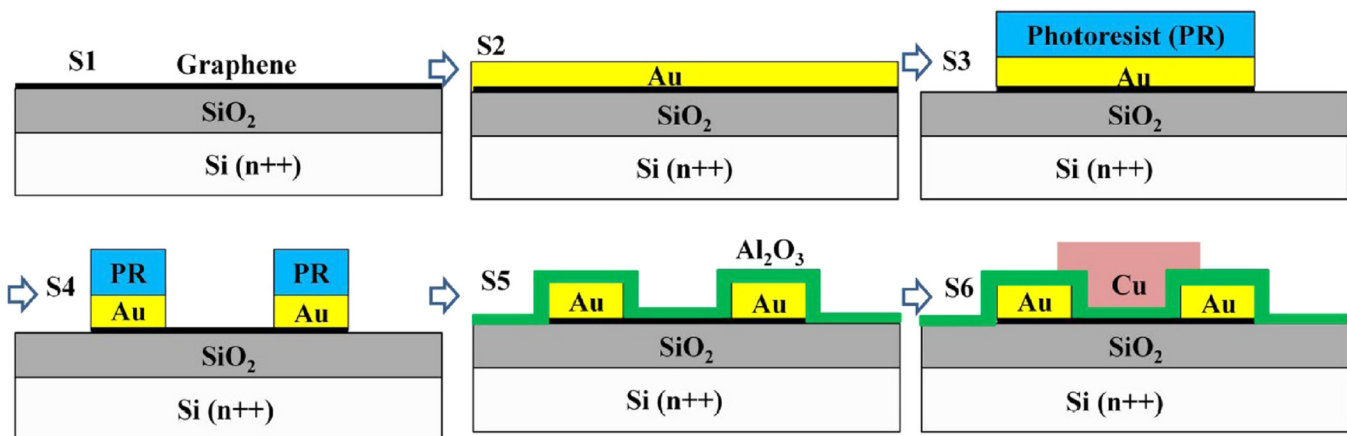


FIG. 14. Schematic for patterning graphene using the photolithography process for fabricating a graphene field effect transistor (GFET). (a) Schematic process flow for a dual gate graphene field effect transistors with key steps from single-layer graphene (SLG) film transfer onto an oxidized Si (n⁺⁺) capped with SiO₂ of 120 or 200 nm in thickness(S1), passivation of the SLG with Au (S2), removal of the unwanted Au and SLG for device isolation (S3), formation of the SLG channel (S4), and atomic layer deposition of Al₂O₃ as the gate dielectric on the SLG channel (S5) to deposition of the top Cu gate electrode (S6). Reproduced from Ahlberg *et al.*, Appl. Phys. Lett. **107**, 203104 (2015), Copyright 2015 AIP Publishing.

of graphene features on a nonsuspended substrate. Typically, a configuration of graphene flakes or thin layers on the surface of the SiO₂-Si substrate is used to fabricate nanoelectronic devices, as shown in Fig. 16.^{81,84–86}

E. Self-assembly

The patterning method through a self-assembly process has been used to fabricate graphene-nanocomposite structures and 3D-graphene structures. Self-assembly is characterized as a bottom up

approach rather than a top-down method which enables a large scale, solution-based process. A self-assembly method typically utilizes surfactants and polymer modified graphene or polymer modified graphene oxide sheets to achieve desired agglomeration properties.^{87–90} It is often used to fabricate self-assembled nanostructures with more complex, multiscale, and multiphase building blocks. Lee *et al.* have reported successful fabrication of microporous 3D carbon films through the use of polymer-grafted GO⁸⁷ as represented in the schematic in Fig. 17. Polymer-grafted GO is dispersed in an organic solvent and then exposed to a stream of humid air. The team was then able to initiate a self-assembly process of aqueous droplets at the surface of an organic solution. Subsequent drying resulted in a microporous film of polymer-grafted GO on the substrate which, upon pyrolysis, formed macroporous films comprising reduced graphene oxide (R-GO) platelets. Yu and Dai also made use of polymer-modified graphene sheets to form graphene/carbon nanotube hybrid carbon films.⁸⁸ Chen *et al.* reported the preparation of magnetic 3D graphene/Fe₃O₄ architectures via an *in-situ* self-assembly process of graphene through mild chemical reduction of graphene oxide in the presence of Fe₃O₄ nanoparticles in water.⁸⁹ Self-assembling ability between anionic surfactants with oppositely charged metal cations was utilized by Wang *et al.* to make ordered metal-oxide-graphene nanocomposites with graphene as fundamental building blocks that contained stable, ordered alternating layers of nanocrystalline metal oxides with graphene or graphene stacks. The ternary self-assembly approach has been utilized to fabricate ordered metal oxide-graphene nanocomposites using surfactants.⁹⁰ Graphene mono-/multilayers are used as substrates for adsorption of anionic sulfonate surfactant hemi-micelles which enables dispersion in an aqueous solution. The self-assembly occurs via the interaction of the anionic sulfonate surfactant on the graphene surface with oppositely charged metal cation (e.g., Sn₂⁺) species, resulting in a transition into lamella mesophase. This lamella mesophase leads to the formation of SnO₂-graphene nanocomposites, where hydrophobic graphene sheets are sandwiched in the hydrophobic domains of the anionic surfactant. Finally, through crystallization of the metal

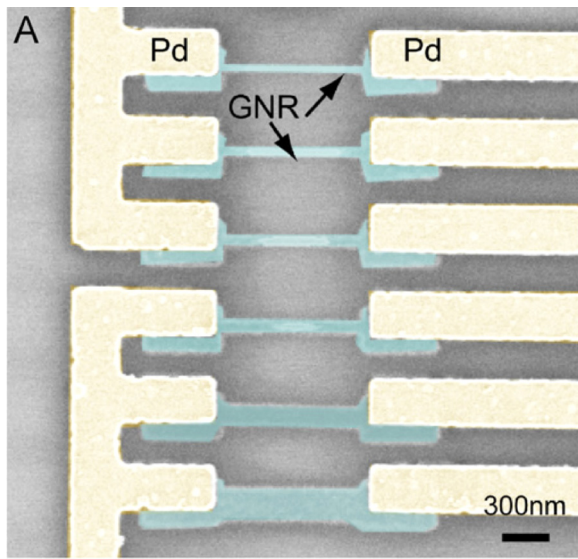


FIG. 15. SEM picture of GNR devices fabricated on a 200-nm SiO₂ substrate. The widths of the GNRs from top to bottom are 20, 30, 40, 50, 100, and 200 nm. Reproduced with permission from Chen *et al.*, Physica E **40**, 228 (2007). Copyright 2007 Elsevier.

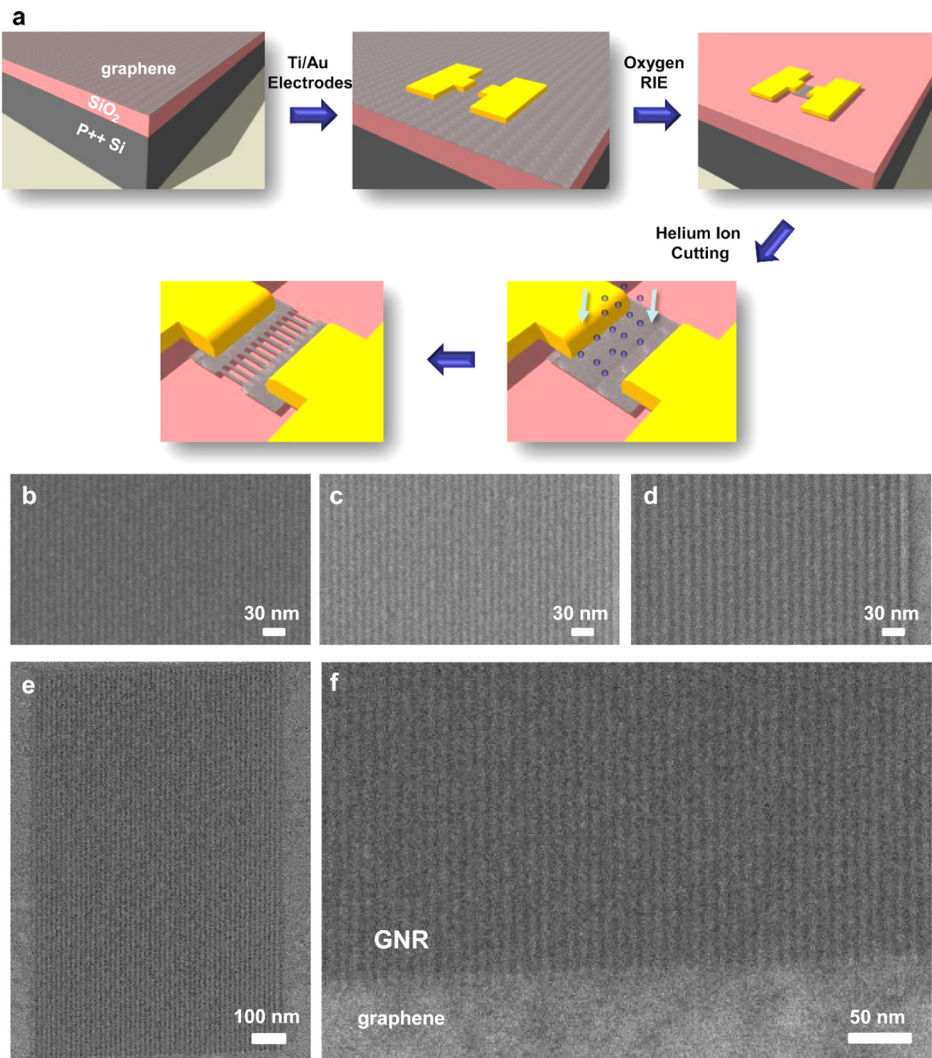


FIG. 16. Graphene nanoribbons (GNRs) patterned with FIB. (a) Schematic of patterning of GNR arrays using helium-ion beam lithography. (b)–(d) He-ion microscopy images of (b) 5 nm, (c) 6 nm, and (d) 7.5 nm half-pitch arrays. (e) He-ion microscopy image of high aspect ratio GNRs (width \times length is 5 nm \times 1200 nm). (f) He-ion microscopy image shows the smooth interface between graphene and patterned GNRs. For all images, bright lines represent graphene. Reproduced with permission from Abbas *et al.*, ACS Nano 8, 1538 (2014). Copyright 2014 American Chemical Society.

oxide and removal of the surfactant, metal oxide-graphene layered nanocomposites are acquired which are composed of alternating layers of metal oxide nanocrystals and graphene/graphene stacks.

F. Direct laser lithography

A focused laser beam can be used to induce photo-reduction of graphene oxide to produce reduced graphene oxide structures. Direct laser lithography techniques have emerged as an appealing alternative because they rely neither on high temperature nor on toxic chemicals as some of the techniques discussed previously and provide direct patterning.⁹⁴ Figure 18 shows some of the direct laser written rGO structures, which are often also referred to as laser scribed graphene (LSG) structures.

It is hypothesized that the photo-reduction mechanism of GO involves a linear absorption accompanied by structural reorganization of the carbon lattice into the planar, hexagonal, and sp^2 graphene structure.^{51,52} While most of the previous photo-reduction methods

utilized UV, Hg, Xe lamps^{94,96} or vis-near IR,^{51,94,97,98} and CO_2 ^{99,100} continuous wave lasers, few work has been done using pulsed lasers. More recently, an increasing number of reports have been presented on patterning graphene using UV^{51,101} and vis-near IR^{51,52,91–93,95,97} pulsed laser systems. These reports suggest that reduction of graphene oxide also occurs through a nonlinear interaction and results in better quality of patterned graphene nano/microstructures. The quality of the structures is analyzed by using several techniques such as comparison of the conductivity values using XPS and Raman measurements, as shown in Figs. 19 and 20, respectively.

Other efforts to achieve better quality direct-laser-written graphene structures include patterning in a liquid nitrogen environment. Guan *et al.* used picosecond pulsed laser irradiation on free-standing GO sheets while immersed in liquid nitrogen at -196°C to freeze the irradiated surface.⁹² The written patterns exhibited better ordered structure with less defects and a crack-free morphology. Localized temperature of laser exposed GO can generate new chemical bonds and have physical interactions with both inorganic and organic

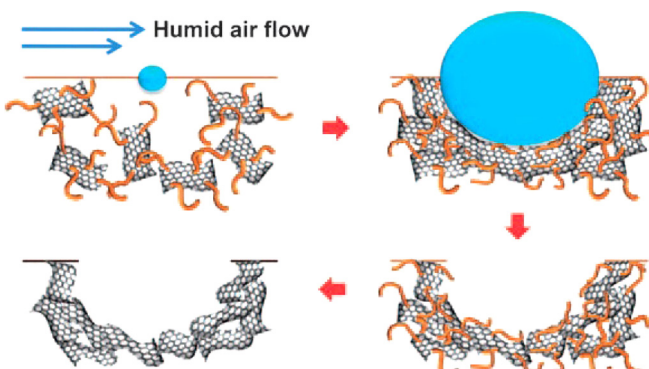


FIG. 17. Procedure for the self-assembly of R-GO into microporous carbon films. Endothermic evaporation of the volatile organic solvent results in a spontaneous condensation and close packing of aqueous droplets at the organic solution surface to produce microporous 3D carbon films. Reproduced with permission from Lee, Angew. Chemie., Int. Ed. **49**, 10084 (2010). Copyright 2010 John Wiley and Sons.

compounds, or destroy the bonds with functional groups attached to the graphene oxide or graphene sheets. This property has been exploited for making various functional devices.^{102–104} 3D micropatterns of graphene have also been achieved with similar protocol of laser patterning but by exposing each layer one at a time followed by spin coating of GO.¹⁰⁵

The laser induced forward transfer (LIFT) technique is another direct laser lithography method to fabricate patterned graphene structures. In LIFT processes, laser pulses initiate propagation of a high velocity microjet of fluid from a thin donor film, of appropriate material, to be deposited onto a receiving substrate. By utilizing a coating of CVD graphene as the donor film, Smits *et al.* have shown successful patterning of graphene structures.⁹³ In another interesting approach, selective graphitization of SiC was performed by ion implantation followed by pulsed laser annealing. Initial work reported by the same

group used Au and Si ion implantation in SiC for eventual graphene formation at low temperature. Later, the modified scheme of ion implantation followed by laser annealing not only allowed selective patterning but also improved electrical performance of Graphene as shown in Fig. 21. This new approach allowed patterning of graphene at much low temperature where Au ions were implanted by the focussed ion beam at low temperature and ambient conditions.^{106,107}

IV. CONCLUSION

Extraordinary properties of graphene make it attractive for applications in optical and electronic devices. Even though several methods for synthesis and processing of graphene exist, there is no single method to suit all purposes. Here, we have reviewed different conventional synthesis and processing techniques along with recently developed patterning methods to design various graphene nano-, micro-, and macrostructures. The review is complemented with inclusion of discussion on the properties. It further highlights the differences of each processing technique and its emerging applications. The fabricated graphene structures exhibit different electrical, mechanical, and thermal properties resulting from structural confinement effects and defects arising from the type of chemical used and the synthesis/fabrication methods. Chemical exfoliation followed by chemical, thermal, or other reduction processes leads to synthesis of rGO. Synthesis of graphene using techniques like CVD produces pristine monolayer or multilayer graphene, as per the requirement. Irradiation processes using an e-beam/ion beam can ablate or exfoliate the GO film surface, while exposure to UV light is expected to undergo the local photothermal reduction effect based on linear absorption. Partial oxidation and photothermal reduction of GO are considered to be main factors for these processes. Decoupling of the photo-thermal phenomenon from the nonthermal phenomenon using pulsed lasers with varying repetition rates presents potential for patterning high quality nanostructures and provides an alternative reduction mechanism of GO using the nonlinear photo-absorption process. Therefore, it is extremely

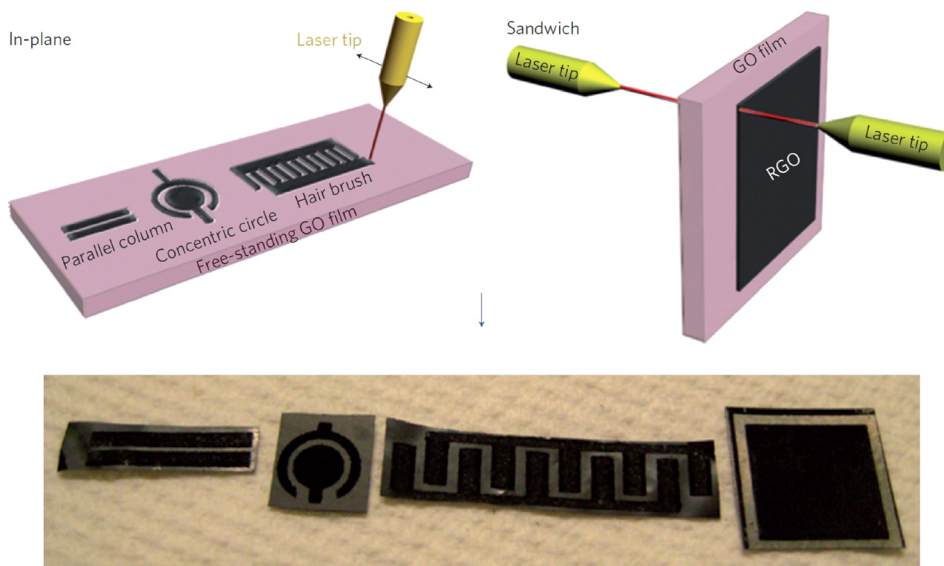


FIG. 18. Schematics of CO_2 laser-patterning of free-standing hydrated GO films to fabricate rGO-GO-rGO devices with in-plane and sandwich geometries.⁹⁹ The black contrast in the top schematics corresponds to rGO and the light contrast to unmodified hydrated GO. For in-plane devices, three different geometries were used, and the concentric circular pattern gives the highest capacitance density. The bottom row shows photographs of patterned films. Reproduced with permission from Gao *et al.*, Nat. Nanotechnol. **6**, 496 (2011). Copyright 2011 Springer Nature.

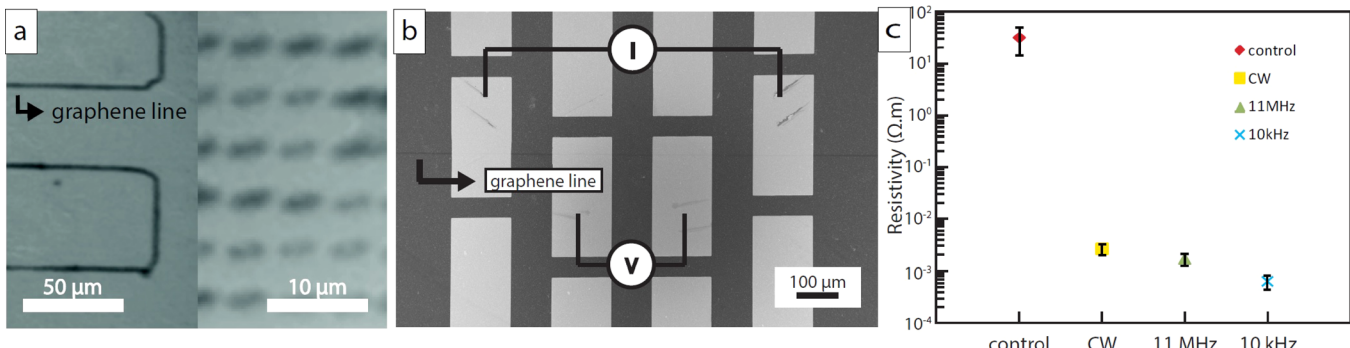


FIG. 19. SEM images of patterned graphene and resistance measurements demonstrating improved conductivity. (a) SEM images of reduced graphene oxide lines (left) and dashes (right). (b) SEM image showing the graphene line with a 4-point probe schematic. Each gold contact is $150\text{ }\mu\text{m} \times 300\text{ }\mu\text{m}$. (c) Resistance of various direct laser written lines (the y axis is on a log scale, and the x axis lists the different types of lasers used). Reproduced with permission from Kang, Opt. Laser Technol. **103**, 340 (2018). Copyright 2018 Elsevier.

important to distinguish the varying properties of the synthesized/patterned graphene which may be extremely crucial for device application.

Most of the synthesis techniques produce graphene in suspended form or on substrates. It is desirable to pattern graphene at specified locations for device fabrication instead of random growth/deposition, for which a combinatorial approach such as self-assembly followed by direct laser lithography or e-beam lithography or by RF plasma treatment in any order/combination holds promising future as proposed in Fig. 22. An insight into the advantages and disadvantages of various techniques/methods that best suit the requirement, in combination or addition of each other, is highly desirable. Although the fundamentals behind the graphene growth and patterning process are not yet fully understood, it is expected that the techniques introduced in this review paper can suggest scientifically interesting and technologically relevant alternative approaches to synthesizing and patterning graphene structures.

V. OUTLOOK

The ability to synthesize and process graphene has been a great driving force in exploration of 2D materials beyond graphene. Theoretical calculations have predicted the availability of a vast two dimensional flatland comprising materials such as Silicene,¹⁰⁸ Germanene,¹⁰⁹ Stanene,¹¹⁰ and metal dichalcogenides,¹¹¹ among

others. These materials are not only expected to provide alternatives to graphene by exhibiting the exotic properties of graphene in parts or entirely but also properties beyond those exhibited by graphene. As an example, the smaller mass of carbon results in negligible spin-orbit coupling which results in almost negligible spin-orbit gap. The spin-orbit coupling is understood to hold the key for preservation of topological states,¹¹² a phenomenon achievable beyond the capabilities of graphene. Therefore, developing an insight into synthesis and processing techniques is important. Motivated by discovery of graphene, chemical and mechanical exfoliation-based techniques have been explored to synthesize/process other 2D materials. These techniques did not evolve as methods of choice due to the limited availability of layered, planar structures stacked via van-der-Waal interactions. Other methods such as ultrahigh vacuum epitaxial growth and vapor deposition have emerged as methods of choice to date to synthesize elemental 2D materials. Another recently explored technique based on ultrafast laser-material interactions using the femto-second laser have also emerged as an alternative inexpensive method to synthesize elemental 2D materials. A significant overlap in synthesis or processing techniques requires a good understanding in furthering the exploration of novel 2D materials toward applications. Thus, an understanding of synthesis and processing procedures on graphene is expected to carry a long way in evolution of futuristic technology based on materials beyond graphene.

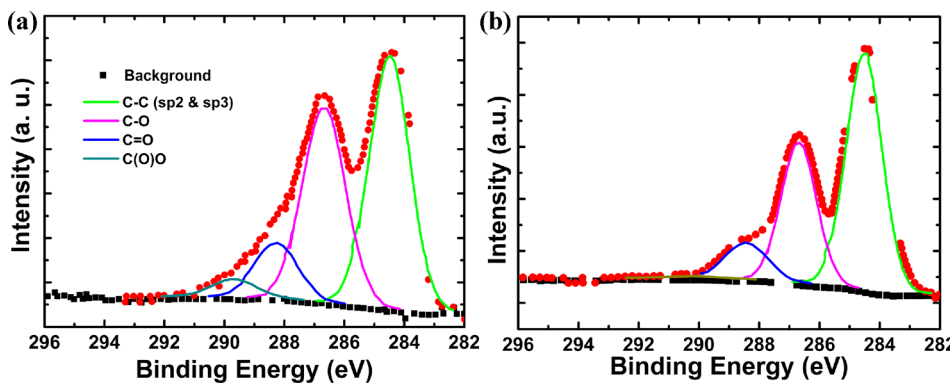


FIG. 20. XPS scans of (a) GO and (b) rGO obtained by irradiating the femtosecond laser (0.15 J cm^{-2} , 40 overlapping pulses). The XPS data was estimated from the data of Ref. 51.

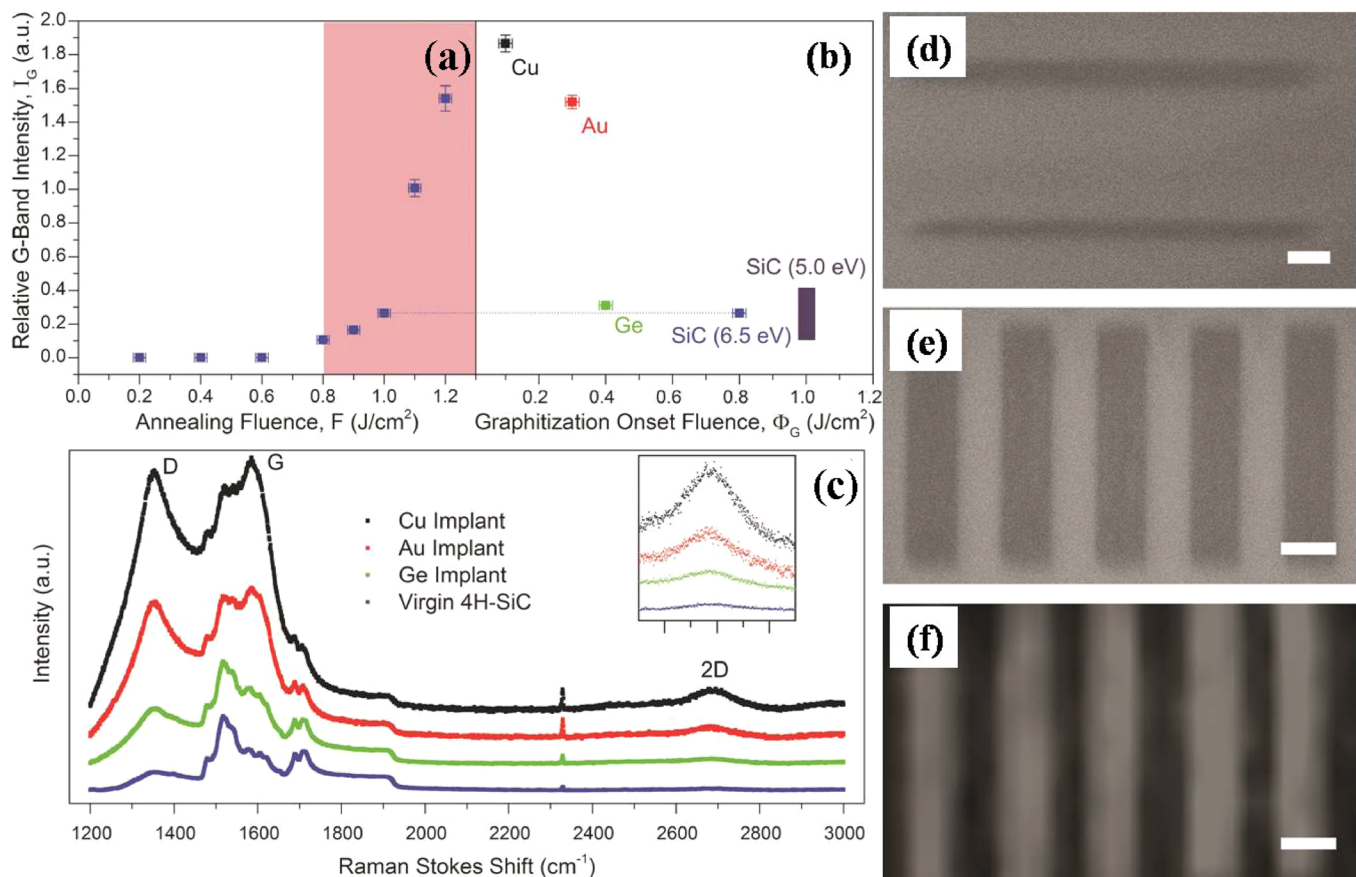


FIG. 21. (a) and (b) Laser fluences on unimplanted SiC and the graphitization for various implanted SiC samples. (c) Raman spectra for each implant condition annealed at $1\text{ J}/\text{cm}^2$ threshold and 50 pulses. The inset shows the zoomed plot of the 2D bands. (d) Growth of FLG with nanoscale features by Au-ion beam lithography and PLA. (e) Reproduction of a plasmonic terahertz metamaterial consisting of a micro-array of $2\text{-}\mu\text{m}$ wide lines. (f) Raman 2D-band map of the metamaterial array. Scale bars are 1, 2, and $2\text{ }\mu\text{m}$, respectively. Reproduced with permission from Lemaitre, Appl. Phys. Lett. **100**, 193105 (2012), Copyright 2012 AIP Publishing.

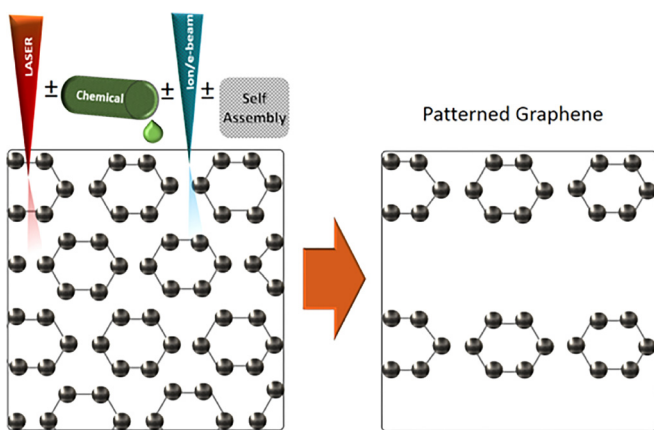


FIG. 22. Schematic showing single or combination of techniques to be used for patterning high quality graphene structures.

REFERENCES

- ¹R. E. Peierls, "Bemerkungen über umwandlungstemperaturen," *Helv. Phys. Acta* **7**, 81 (1934).
- ²L. D. Landau, "Zur Theorie der phasenumwandlungen II," *Phys. Z. Sowjetunion* **11**, 26 (1937).
- ³N. D. Mermin, "Crystalline order in two dimensions," *Phys. Rev.* **176**, 250 (1968).
- ⁴K. S. Novoselov *et al.*, "Electric field effect in atomically thin carbon films," *Science* **306**, 666 (2004).
- ⁵A. K. Geim and I. V. Grigorieva, "Van der Waals heterostructures," *Nature* **499**, 419 (2013).
- ⁶P. R. Wallace, "The band theory of graphite," *Phys. Rev.* **71**, 622 (1947).
- ⁷S. Saxena *et al.*, "Investigation of structural and electronic properties of graphene oxide," *Appl. Phys. Lett.* **99**, 13104 (2011).
- ⁸A. H. Castro Neto, N. M. R. Peres, K. S. Novoselov, A. K. Geim, and F. Guinea, "The electronic properties of graphene," *Rev. Mod. Phys.* **81**, 109 (2009).
- ⁹M. I. Katsnelson, K. S. Novoselov, and A. K. Geim, "Chiral tunnelling and the Klein paradox in graphene," *Nat. Phys.* **2**, 620 (2006).
- ¹⁰M. I. Katsnelson and K. S. Novoselov, "Graphene: New bridge between condensed matter physics and quantum electrodynamics," *Solid State Commun.* **143**, 3 (2007).

- ¹¹T. M. Rusin and W. Zawadzki, "Zitterbewegung of electrons in graphene in a magnetic field," *Phys. Rev. B* **78**, 125419 (2008).
- ¹²V. V. Cheianov and V. I. Fal'ko, "Selective transmission of Dirac electrons and ballistic magnetoresistance of n-p junctions in graphene," *Phys. Rev. B* **74**, 41403 (2006).
- ¹³S. Cho, Y.-F. Chen, and M. S. Fuhrer, "Gate-tunable graphene spin valve," *Appl. Phys. Lett.* **91**, 123105 (2007).
- ¹⁴J. Chang, G. Zhou, E. R. Christensen, R. Heideman, and J. Chen, "Graphene-based sensors for detection of heavy metals in water: A review," *Anal. Bioanal. Chem.* **406**, 3957 (2014).
- ¹⁵P. B. Pawar *et al.*, "Water Purification using Graphene covered micro-porous, reusable carbon membrane," *MRS Adv.* **1**, 1411 (2016).
- ¹⁶A. Pandey *et al.*, "3D oxidized graphene frameworks: An efficient adsorbent for methylene blue," *J. Miner.* **70**, 469 (2018).
- ¹⁷G. Eda, H. Emrah Unalan, N. Rupesinghe, G. A. J. Amaralunga, and M. Chhowalla, "Field emission from graphene based composite thin films," *Appl. Phys. Lett.* **93**, 233502 (2008).
- ¹⁸M. Pumera, "Graphene in biosensing," *Mater. Today* **14**, 308 (2011).
- ¹⁹R. P. Choudhary, S. Shukla, K. Vaibhav, P. B. Pawar, and S. Sumit, "Optical properties of few layered graphene quantum dots," *Mater. Res. Express* **2**, 95024 (2015).
- ²⁰S. Shukla and S. Saxena, "Spectroscopic investigation of confinement effects on optical properties of graphene oxide," *Appl. Phys. Lett.* **98**, 73104 (2011).
- ²¹X. Wang, L. Zhi, and K. Müllen, "Transparent, conductive graphene electrodes for dye-sensitized solar cells," *Nano Lett.* **8**, 323 (2008).
- ²²A. K. Geim and K. S. Novoselov, "The rise of graphene," *Nat. Mater.* **6**, 183 (2007).
- ²³B. Partoens and F. Peeters, "From graphene to graphite: Electronic structure around the K point," *Phys. Rev. B* **74**, 075404 (2006).
- ²⁴S. Morozov *et al.*, "Two-dimensional electron and hole gases at the surface of graphite," *Phys. Rev. B* **72**, 201401 (2005).
- ²⁵B. Lang, "A LEED study of the deposition of carbon on platinum crystal surfaces," *Surf. Sci.* **53**, 317 (1975).
- ²⁶A. Nagashima *et al.*, "Electronic structure of monolayer graphite on some transition metal carbide surfaces," *Surf. Sci.* **287–288**, 609 (1993).
- ²⁷H. Shioyama, "Cleavage graphite to graphene," *J. Mater. Sci. Lett.* **20**, 499 (2001).
- ²⁸L. M. Viculis, J. J. Mack, and R. B. Kaner, "A chemical route to carbon nanoscrolls," *Science* **299**, 1361 (2003).
- ²⁹M. Yi and Z. Shen, "A review on mechanical exfoliation for the scalable production of graphene," *J. Mater. Chem. A* **3**, 11700 (2015).
- ³⁰B. Jayasena and S. Subbiah, "A novel mechanical cleavage method for synthesizing few-layer graphenes," *Nanoscale Res. Lett.* **6**, 95 (2011).
- ³¹M. Lotya *et al.*, "Liquid phase production of graphene by exfoliation of graphite in surfactant/water solutions," *J. Am. Chem. Soc.* **131**, 3611 (2009).
- ³²Y. Hernandez *et al.*, "High-yield production of graphene by liquid-phase exfoliation of graphite," *Nat. Nanotechnol.* **3**, 563 (2008).
- ³³J. N. Coleman, "Liquid exfoliation of defect-free graphene," *Acc. Chem. Res.* **46**, 14 (2013).
- ³⁴X. Wang *et al.*, "Heteroatom doped graphene materials: Syntheses, properties and applications," *Chem. Soc. Rev.* **43**, 7067 (2014).
- ³⁵A. E. Karu and M. Beer, "Pyrolytic formation of highly crystalline graphite films," *J. Appl. Phys.* **37**, 2179 (1966).
- ³⁶X. Li *et al.*, "Large-area synthesis of high-quality and uniform graphene films on copper foils," *Science* **324**, 1312 (2009).
- ³⁷E. S. Polsen, D. Q. McNerny, B. Viswanath, S. W. Pattinson, and A. John Hart, "High-speed roll-to-roll manufacturing of graphene using a concentric tube CVD reactor," *Sci. Rep.* **5**, 10257 (2015).
- ³⁸J. C. Shelton, H. R. Patil, and J. M. Blakely, "Equilibrium segregation of carbon to a nickel (111) surface: A surface phase transition," *Surf. Sci.* **43**, 493 (1974).
- ³⁹M. A. Capano, B. M. Capano, D. T. Morisette, A. Salleo, S. Lee, and M. F. Toney, "High-resolution x-ray analysis of graphene grown on 4H-SiC (000 1) at low pressures," *J. Mater. Res.* **29**, 439 (2014).
- ⁴⁰C. Berger *et al.*, "Ultrathin epitaxial graphite: 2D electron gas properties and a route toward graphene-based nanoelectronics," *J. Phys. Chem. B* **108**, 19912 (2004).
- ⁴¹W. S. Hummers and R. E. Offeman, "Preparation of graphitic oxide," *J. Am. Chem. Soc.* **80**, 1339 (1958).
- ⁴²D. C. Marcano *et al.*, "Improved synthesis of graphene oxide," *ACS Nano* **4**, 4806 (2010).
- ⁴³S. Park *et al.*, "Colloidal suspensions of highly reduced graphene oxide in a wide variety of organic solvents," *Nano Lett.* **9**, 1593 (2009).
- ⁴⁴L. L. Zhang, R. Zhou, and X. S. Zhao, "Graphene-based materials as supercapacitor electrodes," *J. Mater. Chem.* **20**, 5983 (2010).
- ⁴⁵F. Miao *et al.*, "Inkjet printing of electrochemically-exfoliated graphene nanoplatelets," *Synth. Met.* **220**, 318 (2016).
- ⁴⁶A. G. Cano-Márquez *et al.*, "Ex-MWNTs: Graphene sheets and ribbons produced by lithium intercalation and exfoliation of carbon nanotubes," *Nano Lett.* **9**, 1527 (2009).
- ⁴⁷L. Jiao, L. Zhang, X. Wang, G. Diankov, and H. Dai, "Narrow graphene nano-ribbons from carbon nanotubes," *Nature* **458**, 877 (2009).
- ⁴⁸D. V. Kosynkin *et al.*, "Longitudinal unzipping of carbon nanotubes to form graphene nanoribbons," *Nature* **458**, 872 (2009).
- ⁴⁹B. Rethfeld, D. S. Ivanov, M. E. Garcia, and S. I. Anisimov, "Modelling ultra-fast laser ablation," *J. Phys. D: Appl. Phys.* **50**, 193001 (2017).
- ⁵⁰M. Qian *et al.*, "Formation of graphene sheets through laser exfoliation of highly disordered pyrolytic graphite," *Appl. Phys. Lett.* **98**, 173108 (2011).
- ⁵¹R. Arul *et al.*, "The mechanism of direct laser writing of graphene features into graphene oxide films involves photoreduction and thermally assisted structural rearrangement," *Carbon* **99**, 423 (2016).
- ⁵²S. Kang, C. C. Evans, S. Shukla, O. Reshef, and E. Mazur, "Patterning and reduction of graphene oxide using femtosecond-laser irradiation," *Opt. Laser Technol.* **103**, 340 (2018).
- ⁵³Y. Miyamoto, H. Zhang, and D. Tománek, "Photoexfoliation of graphene from graphite: An *ab initio* study," *Phys. Rev. Lett.* **104**, 208302 (2010).
- ⁵⁴W. Zhang *et al.*, "A strategy for producing pure single-layer graphene sheets based on a confined self-assembly approach," *Angew. Chem., Int. Ed.* **48**, 5864 (2009).
- ⁵⁵W. Nie *et al.*, "Three-dimensional porous scaffold by self-assembly of reduced graphene oxide and nano-hydroxyapatite composites for bone tissue engineering," *Carbon* **116**, 325 (2017).
- ⁵⁶X. Liu *et al.*, "Graphene nanowires anchored to 3D graphene foam via self-assembly for high performance Li and Na ion storage," *Nano Energy* **37**, 108 (2017).
- ⁵⁷C. Yunfeng *et al.*, "Self-Assembly of flexible free-standing 3D porous MoS₂-reduced graphene oxide structure for high-performance lithium-ion batteries," *Adv. Funct. Mater.* **27**, 1700234 (2017).
- ⁵⁸Q. Bao and K. P. Loh, "Graphene photonics, plasmonics, and broadband optoelectronic devices," *ACS Nano* **6**, 3677 (2012).
- ⁵⁹G. Xiong, C. Meng, R. G. Reifenberger, P. P. Irazoqui, and T. S. Fisher, "A review of graphene-based electrochemical microsupercapacitors," *Electroanalysis* **26**, 30 (2014).
- ⁶⁰S. Santra *et al.*, "CMOS integration of inkjet-printed graphene for humidity sensing," *Sci. Rep.* **5**, 17374 (2015).
- ⁶¹M. H. Ervin, L. T. Le, and W. Y. Lee, "Inkjet-printed flexible graphene-based supercapacitor," *Electrochim. Acta* **147**, 610 (2014).
- ⁶²S. Majee, C. Liu, B. Wu, S. L. Zhang, and Z. B. Zhang, "Ink-jet printed highly conductive pristine graphene patterns achieved with water-based ink and aqueous doping processing," *Carbon* **114**, 77 (2017).
- ⁶³W. S. Chang *et al.*, "Micropatterning of reduced graphene oxide by meniscus-guided printing," *Carbon* **123**, 364 (2017).
- ⁶⁴E. B. Secor, B. Y. Ahn, T. Z. Gao, J. A. Lewis, and M. C. Hersam, "Rapid and versatile photonic annealing of graphene inks for flexible printed electronics," *Adv. Mater.* **27**, 6683 (2015).
- ⁶⁵A. Capasso *et al.*, "Ink-jet printing of graphene for flexible electronics: An environmentally-friendly approach," *Solid State Commun.* **224**, 53 (2015).
- ⁶⁶C. Zhu *et al.*, "Highly compressible 3D periodic graphene aerogel micro-lattices," *Nat. Commun.* **6**, 6962 (2015).
- ⁶⁷A. E. Jakus *et al.*, "Three-dimensional printing of high-content graphene scaffolds for electronic and biomedical applications," *ACS Nano* **9**, 4636 (2015).
- ⁶⁸W. J. Hyun, E. B. Secor, M. C. Hersam, C. D. Frisbie, and L. F. Francis, "High-resolution patterning of graphene by screen printing with a silicon stencil for highly flexible printed electronics," *Adv. Mater.* **27**, 109 (2015).

- ⁶⁹Z. Liu *et al.*, "Ultraflexible in-plane micro-supercapacitors by direct printing of solution-processable electrochemically exfoliated graphene," *Adv. Mater.* **28**, 2217 (2016).
- ⁷⁰Z.-S. Wu, K. Parvez, X. Feng, and K. Müllen, "Photolithographic fabrication of high-performance all-solid-state graphene-based planar micro-supercapacitors with different interdigital fingers," *J. Mater. Chem. A* **2**, 8288 (2014).
- ⁷¹P. Ahlberg *et al.*, "A two-in-one process for reliable graphene transistors processed with photo-lithography," *Appl. Phys. Lett.* **107**, 203104 (2015).
- ⁷²J. W. Shin *et al.*, "Display process compatible accurate graphene patterning for OLED applications," *2D Materials* **5**, 014003 (2018).
- ⁷³R. Shi, H. Xu, B. Chen, Z. Zhang, and L. Peng, "Scalable fabrication of graphene devices through photolithography," *Appl. Phys. Lett.* **102**, 113102 (2013).
- ⁷⁴X. Wang and H. Dai, "Etching and narrowing of graphene from the edges," *Nat. Chem.* **2**, 661 (2010).
- ⁷⁵J. W. Suk *et al.*, "Transfer of CVD-grown monolayer graphene onto arbitrary substrates," *ACS Nano* **5**, 6916 (2011).
- ⁷⁶X. Liang *et al.*, "Toward clean and crackless transfer of graphene," *ACS Nano* **5**, 9144 (2011).
- ⁷⁷Y. Lee *et al.*, "Wafer-scale synthesis and transfer of monolayer graphene," *Nano Lett.* **10**, 490 (2010).
- ⁷⁸M. D. Fischbein and M. Drndić, "Electron beam nanosculpting of suspended graphene sheets," *Appl. Phys. Lett.* **93**, 113107 (2008).
- ⁷⁹Z. Chen, Y. M. Lin, M. J. Rooks, and P. Avouris, "Graphene nano-ribbon electronics," *Phys. E* **40**, 228 (2007).
- ⁸⁰L. Tapaszti, G. Dobrik, P. Lambin, and L. P. Biró, "Tailoring the atomic structure of graphene nanoribbons by scanning tunnelling microscope lithography," *Nat. Nanotechnol.* **3**, 397 (2008).
- ⁸¹S. A. Boden, Z. Moktadir, D. M. Bagnall, H. Mizuta, and H. N. Rutt, "Focused helium ion beam milling and deposition," *Microelectron. Eng.* **88**, 2452 (2011).
- ⁸²J. F. Doyen *et al.*, "Side-gated transport in focused-ion-beam-fabricated multi-layered graphene nanoribbons," *Small* **4**, 716 (2008).
- ⁸³D. Lucot *et al.*, "Deposition and FIB direct patterning of nanowires and nanorings into suspended sheets of graphene," *Microelectron. Eng.* **86**, 882 (2009).
- ⁸⁴A. N. Abbas *et al.*, "Patterning, characterization, and chemical sensing applications of graphene nanoribbon arrays down to 5 nm using helium ion beam lithography," *ACS Nano* **8**, 1538 (2014).
- ⁸⁵N. Kalhor, S. A. Boden, and H. Mizuta, "Sub-10 nm patterning by focused He-ion beam milling for fabrication of downscaled graphene nano devices," *Microelectron. Eng.* **114**, 70 (2014).
- ⁸⁶D. C. Bell, M. C. Lemme, L. A. Stern, J. R. Williams, and C. M. Marcus, "Precision cutting and patterning of graphene with helium ions," *Nanotechnology* **20**, 455301 (2009).
- ⁸⁷S. H. Lee *et al.*, "Three-dimensional self-assembly of graphene oxide platelets into mechanically flexible macroporous carbon films," *Angew. Chem., Int. Ed.* **49**, 10084 (2010).
- ⁸⁸D. Yu and L. Dai, "Self-assembled graphene/carbon nanotube hybrid films for supercapacitors," *J. Phys. Chem. Lett.* **1**, 467 (2010).
- ⁸⁹W. Chen, S. Li, C. Chen, and L. Yan, "Self-assembly and embedding of nanoparticles by in situ reduced graphene for preparation of a 3D graphene/nano-particle aerogel," *Adv. Mater.* **23**, 5679 (2011).
- ⁹⁰D. Wang *et al.*, "Ternary self-assembly of ordered metal oxide - graphene nanocomposites for electrochemical energy storage," *ACS Nano* **4**, 1587 (2010).
- ⁹¹R.-Z. Li *et al.*, "High-rate in-plane micro-supercapacitors scribed onto photo paper using in situ femtolaser-reduced graphene oxide/Au nanoparticle microelectrodes," *Energy Environ. Sci.* **9**, 1458 (2016).
- ⁹²Y. C. Guan, Y. W. Fang, G. C. Lim, H. Y. Zheng, and M. H. Hong, "Fabrication of laser-reduced graphene oxide in liquid nitrogen environment," *Sci. Rep.* **6**, 28913 (2016).
- ⁹³E. C. P. Smits *et al.*, "Laser induced forward transfer of graphene Laser induced forward transfer of graphene," *Appl. Phys. Lett.* **111**, 173101 (2017).
- ⁹⁴Y.-L. Zhang *et al.*, "Photoreduction of graphene oxides: Methods, properties, and applications," *Adv. Opt. Mater.* **2**, 10 (2014).
- ⁹⁵Y. Zhang *et al.*, "Direct imprinting of microcircuits on graphene oxides film by femtosecond laser reduction," *Nano Today* **5**, 15 (2010).
- ⁹⁶G. Williams, B. Seger, and P. V. Kamat, "UV-assisted photocatalytic reduction of graphene oxide," *ACS Nano* **2**, 1487 (2008).
- ⁹⁷D. A. Sokolov, K. R. Shepperd, and T. M. Orlando, "Formation of graphene features from direct laser-induced reduction of graphite oxide," *J. Phys. Chem. Lett.* **1**, 2633 (2010).
- ⁹⁸M. F. El-Kady, V. Strong, S. Dubin, and R. B. Kaner, "Laser scribing of high-performance and flexible graphene-based electrochemical capacitors," *Science* **335**, 1326 (2012).
- ⁹⁹W. Gao *et al.*, "Direct laser writing of micro-supercapacitors on hydrated graphite oxide films," *Nat. Nanotechnol.* **6**, 496 (2011).
- ¹⁰⁰R. Mukherjee, A. V. Thomas, A. Krishnamurthy, and N. Koratkar, "Photothermally reduced graphene as high-power anodes for lithium-ion Batteries," *ACS Nano* **6**, 7867 (2012).
- ¹⁰¹D. A. Sokolov, C. M. Rouleau, D. B. Geohegan, and T. M. Orlando, "Excimer laser reduction and patterning of graphite oxide," *Carbon* **53**, 81 (2013).
- ¹⁰²C. Huhu *et al.*, "Graphene fibers with predetermined deformation as moisture-triggered actuators and robots," *Angew. Chem. Int. Ed.* **52**, 10482 (2013).
- ¹⁰³X. Shi *et al.*, "Femtosecond laser rapid fabrication of large-area rose-like micropatterns on free standing flexible graphene films," *Sci. Rep.* **5**, 17557 (2015).
- ¹⁰⁴V. Strong *et al.*, "Patterning and electronic tuning of laser scribed graphene for flexible all-carbon devices," *ACS Nano* **6**, 1395 (2012).
- ¹⁰⁵H. Fatt Teoh, Y. Tao, E. Soon Tok, G. Wei Ho, and C. Haur Sow, "Direct laser-enabled graphene oxide-reduced graphene oxide layered structures with micropatterning," *J. Appl. Phys.* **112**, 64309 (2012).
- ¹⁰⁶S. Tongay *et al.*, "Drawing graphene nanoribbons on SiC by ion implantation," *Appl. Phys. Lett.* **100**, 073501 (2012).
- ¹⁰⁷M. G. Lemaitre *et al.*, "Low-temperature, site selective graphitization of SiC via ion implantation and pulsed laser annealing," *Appl. Phys. Lett.* **100**, 193105 (2012).
- ¹⁰⁸J. Zhao *et al.*, "Rise of silicene: A competitive 2D material," *Prog. Mater. Sci.* **83**, 24 (2016).
- ¹⁰⁹M. E. Dávila and G. Le Lay, "Few layer epitaxial germanene: A novel two-dimensional Dirac material," *Sci. Rep.* **6**, 20714 (2016).
- ¹¹⁰S. Saxena, R. P. Chaudhary, and S. Shukla, "Stanene: Atomically thick free-standing layer of 2D hexagonal tin," *Sci. Rep.* **6**, 31073 (2016).
- ¹¹¹R. K. Joshi *et al.*, "Hydrogen generation via photoelectrochemical water splitting using chemically exfoliated MoS₂ layers," *AIP Adv.* **6**, 15315 (2016).
- ¹¹²F. Matusalem, D. S. Koda, F. Bechstedt, M. Marques, and L. K. Teles, "Deposition of topological silicene, germanene and stanene on graphene-covered SiC substrates," *Sci. Rep.* **7**, 15700 (2017).